Cardiac Magnetic Resonance

Noninvasive Detection of Myocardial Fibrosis in Arrhythmogenic Right Ventricular Cardiomyopathy Using Delayed-Enhancement Magnetic Resonance Imaging

Harikrishna Tandri, MD,* Manoj Saranathan, PHD,† E. Rene Rodriguez, MD,* Claudia Martinez, MD,*
Chandra Bomma, MD,* Khurram Nasir, MBBS,* Boas Rosen, MD,* João A. C. Lima, MD,*
Hugh Calkins, MD,* David A. Bluemke, MD, PHD*†

Baltimore, Maryland

OBJECTIVES	We evaluated the role of myocardial delayed-enhancement (MDE) magnetic resonance imaging (MRI) for noninvasive detection of fibrosis in Arrhythmogenic right ventricular dysplasia/cardiomyopathy (ARVD/C).
BACKGROUND	Arrhythmogenic right ventricular dysplasia/cardiomyopathy is characterized by fibro-fatty replacement of the right ventricle (RV) leading to arrhythmias and RV failure. Endomyocardial biopsy can demonstrate fibro-fatty replacement of the RV myocardium; however, the test is invasive and carries a risk of perforation.
METHODS	Thirty consecutive patients were prospectively evaluated for ARVD/C. Magnetic resonance imaging was performed on a 1.5-T scanner. Ten minutes after intravenous administration of 0.2 mmol/kg of gadodiamide, MDE-MRI was obtained. Diagnosis of ARVD/C was based upon the Task Force criteria and did not include MRI findings.
RESULTS	Twelve (40%) of 30 patients met the Task Force criteria for ARVD/C. Eight (67%) of the 12 ARVD/C patients demonstrated increased signal on MDE-MRI in the RV compared with none (0%) of the 18 patients without ARVD/C (p < 0.001). Endomyocardial biopsy was performed in 9 of the 12 ARVD/C patients. Of the nine patients, four had fibro-fatty changes consistent with the diagnosis of ARVD/C. Each of these patients had increased RV signal on MDE-MRI. None of the patients without ARVD/C had any abnormalities either on histopathology or on MDE-MRI. Electrophysiologic testing revealed inducible sustained ventricular tachycardia (VT) in six of the eight ARVD/C patients with delayed enhancement, compared with none of the ARVD/C patients without delayed enhancement (p = 0.01).
CONCLUSIONS	Noninvasive detection of RV myocardial fibro-fatty changes in ARVD/C is possible by MDE-MRI. Magnetic resonance imaging findings had an excellent correlation with histopathology and predicted inducible VT on programmed electrical stimulation, suggesting a possible role in evaluation and diagnosis of patients with suspected ARVD/C. (J Am Coll Cardiol 2005;45:98–103) © 2005 by the American College of Cardiology Foundation

Arrhythmogenic right ventricular dysplasia/cardiomyopathy (ARVD/C) is characterized by structural and functional abnormalities of the right ventricular (RV) leading to ventricular arrhythmias and progressive RV failure. The most striking morphological feature of ARVD/C is diffuse or segmental replacement of myocardium in the RV free wall by fibro-fatty tissue (1–3). Diagnosis of ARVD/C at its early stages remains a clinical challenge (4,5), more so in patients with minimal RV abnormalities at echocardiographic or angiographic examination. Endomyocardial biopsy has the potential for in vivo demonstration of typical fibro-fatty replacement of the RV myocardium. However, sensitivity of this test is low because, for reasons of safety, biopsy samples are usually taken from the septum, a region uncommonly involved by the disease (6).

Magnetic resonance imaging (MRI) is a promising technique for delineation of RV anatomy and function as well as for characterizing the composition of the RV wall, especially with regard to the presence of fatty tissue (7,8). However, fat visualization on MRI has not been found to be specific for ARVD (9,10), and there is poor inter-reader agreement in reporting of fat (11). Recently, myocardial delayed enhancement (MDE) after intravenous administration of a gadolinium-based contrast agent has been shown in dysfunctional areas of the left ventricle in patients with prior myocardial infarction and fibrous scar (12,13). We hypothesized that the RV in ARVD/C patients will demonstrate increased signal on MDE-MRI because of the fibrotic nature of the disease process.

METHODS

The study population included 30 patients who were prospectively evaluated for possible ARVD/C because of either a family history or left bundle branch block (LBBB) morphology ventricular arrhythmia. Each of these patients

was evaluated with a detailed clinical history, physical examination, electrocardiogram (ECG), signal-averaged ECG, two-dimensional echocardiography, and contrast-enhanced cardiac MRI. Invasive testing, including electrophysiologic (EP) testing, right ventriculography, and endomyocardial biopsy, was performed guided by the results of noninvasive testing. Final diagnosis of ARVD/C was made independently of the MRI findings. The results of delayed-enhancement MRI were then correlated with the final diagnoses and the results of endomyocardial biopsy. The study was approved by our institutional review board, and informed consent was obtained from the study subjects.

MRI protocol. The MRI examination was performed with a 1.5-T MR imager (CV/I, General Electric Medical Systems, Waukesha, Wisconsin) using a dedicated phased-array cardiac coil. Transaxial black blood images were acquired using a double-inversion recovery (blood suppression) fast-spin echo sequence (time to repetition [TR] = 1 R-R interval, time to echo [TE] = 5 ms, slice thickness = 5 mm, interslice gap = 5 mm, and field of view [FOV] = 24 to 28 cm). Following this, the same sequence was repeated with the chemical shift fat suppression manually tuned to the fat peak to generate fat-suppressed axial black blood images. Bright blood cine imaging in the axial and short-axis planes was acquired by a steady-state, free-precession pulse sequence (TR = 3.5, TE = 1.2 ms, flip angle = 45°, slice thickness = 8 mm, interslice gap = 4 mm, and FOV = 36 to 40 cm, 10 views per segment, 35 ms temporal resolution per cine phase). After intravenous administration of an MRI contrast agent (0.2 mmol/kg of gadodiamide [Omniscan, Amersham Health, Princeton, New Jersey]), inversion recovery prepared breath-hold cine gradient-echo images were obtained 20 min after contrast agent injection. Initially, three-dimensional inversion recovery prepared breath-hold, fat-suppressed, gradient-echo imaging was performed in the short axis and axial planes. The use of a variable sampling in time segmentation (14) scheme enabled the acquisition of three-dimensional volumes in a single 24-heartbeat breath-hold. For three-dimensional im-

aging, the parameters were as follows: TR/TE = 4.7 ms/1.7 ms, flip angle = 20°, slice thickness = 5 to 7 mm, matrix = 256×160, half Fourier acquisition, 12 slices interpolated to 24, FOV = 360×270 mm. A single three-dimensional slab encompassed both ventricles. This was followed by breath-hold two-dimensional imaging (7.2/3.2; inversion time optimized 150 to 200 ms; flip angle = 25°; slice thickness = 8 mm; slice gap = 2 mm; number of excitations = 2; matrix = 256×192; and FOV = 360×270 mm). The two-dimensional MDE MRI scans were obtained in the short axis and axial planes at 10-mm intervals covering the entire right and left ventricles.

Image analysis. The RV was divided into three levels in the short-axis plane: basal, mid, and apical. Each of these three levels was further divided into three segments (superior, midwall, inferior), resulting in a nine-segment model for the RV. Gadolinium enhancement was assessed in each of these segments by observers who had no knowledge of clinical information, using the following scale: 0 = none and 1 = presence of delayed enhancement. The segment scores were summed, yielding a range per patient of 0 (no enhancement in any slice) to 9.

The contrast-to-noise ratio (CNR) of the RV free wall was evaluated as follows: a region of interest (ROI) with a size of 0.1 to 0.2 cm^2 was placed within the RV wall in the zone of increased signal intensity. A second ROI of identical size was placed within the nearest zone of the RV free wall showing normal-appearing myocardium. The difference between the mean signal intensities of both ROIs was then divided by the standard deviation of the background noise signal (ROI = 2 cm^2) measured anteriorly to the RV.

Global ventricular volumes were calculated from the short-axis cine images using a summation of disks method ("Simpson's Rule"), with integration over the image slices using the software program MASS (Medis, Leiden, The Netherlands).

Endomyocardial biopsy. Biopsy specimens were taken from the myocardial border of the interventricular septum, with the use of modified Stanford-Caves bioptome (Scholten Surgical, Redwood City, California), by way of the right internal jugular vein. At least five specimens were obtained from each patient, immediately fixed in 10% formalin, embedded in paraffin, sectioned, stained with hematoxylin and eosin, and reviewed at a minimum of four section levels by one cardiac pathologist. The reviewing pathologist was not aware of the clinical characteristics of the patients. A percentage of fat >3% and of fibrous tissue >40% with <45% myocytes was considered diagnostic of ARVD/C (6).

EP study protocol. A standardized EP study was performed in all patients. A conventional stimulation protocol was used with one, two, and three extrastimuli delivered at three drive train cycle lengths at the RV apex and RV outflow tract. Burst pacing at cycle lengths from 600 to 300 ms was also used. Testing was performed in the baseline state and during a 2 μ/min infusion of isoproterenol. A study was considered positive if sustained monomorphic ventricular tachycardia (VT) was induced (VT with uniform

Table 1. Clinical Characteristics of Patients With ARVD

			ECG				RV Angiography		
Case	Age/ Gender	Family History	T-Wave Inversions	SAECG	Arrhythmia	Holter	RVD	Aneurysm/ Dyskinesia	Biopsy
1	40/M	No	RBBB	AB	none	NSVT	severe	anterior/RVOT	fibro-fatty
2	45/F	No	$V_1–V_3$	N	SVT	SVT	mild	none	fibro-fatty
3	35/F	Yes	$V_1–V_5$	AB	SVT	ND	severe	anterior	fibro-fatty
4	16/M	Yes	$V_1–V_5$	N	none	normal	mild	basal	normal
5	46/F	No	$V_1–V_4$	AB	none	NSVT	none	basal	ND
6	31/F	No	$V_1–V_3$	AB	SVT	11,000 PVCs	mild	none	ND
7	31/F	Yes	$V_1–V_4$	N	none	350 PVCs	mild	none	normal
8	30/M	No	$V_1–V_5$	AB	SVT	ND	mild	RVOT	normal
9	21/F	Yes	$V_1–V_4$	N	none	700 PVCs	none	normal	normal
10	47/F	Yes	$V_1–V_4$	N	none	normal	none	basal	ND
11	23/M	No	$V_1–V_4$	AB	SVT	ND	moderate	anterior/RVOT	myocarditis
12	58/M	No	$V_1–V_6$	AB	SVT	ND	severe	basal	fibrosis

ARVD = arrhythmogenic right ventricular dysplasial cardiomyopathy; ECG = electrocardiogram; mild RVD = right ventricular ejection fraction 40% to 55%; ND = not done; NS = no symptoms; NSVT = non-sustained ventricular tachycardia; PVC = premature ventricular contraction; RBBB = right bundle branch block; RV = right ventricle; RVD = right ventricular dysfunction; SAECG = signal-averaged electrocardiogram; severe RVD = right ventricular ejection fraction <35%; SVT = sustained ventricular tachycardia.

QRS configuration and cycle length >200 ms lasting 30 s or requiring termination because of hemodynamic compromise). The EP study was negative if the stimulation protocol was completed without induction of sustained VT. Induction of non-sustained ventricular tachycardia (NSVT) and ventricular fibrillation were considered nonspecific findings.

Statistical analyses. The data are presented as mean ± standard deviation. The Mann-Whitney *U* test and Fisher exact test was performed where appropriate. Spearman correlation coefficient was used for correlation analyses. A p value of <0.05 was considered statistically significant.

RESULTS

The mean age was 35 ± 12 years, and 60% (18) of the patients were female. Nine patients (30%) were evaluated because of a family history of ARVD/C, and the others presented with LBBB morphology VT (sustained [n = 6] and nonsustained [n = 15]). None of the patients had a prior history of coronary artery disease, diabetes, or hypertension. Coronary angiography performed in 14 (47%) of the 30 patients upon discretion of their attending cardiologist revealed no significant coronary artery disease. Left ventricular function assessed on echocardiography was nor-

mal in all patients. None of the patients had evidence of pulmonary hypertension on Doppler echocardiography. Twelve (40%) of the 30 patients met the Task Force criteria and were eventually diagnosed with ARVD/C. The clinical characteristics of the 12 patients with ARVD/C are shown in Table 1. The remaining 18 patients had structurally normal hearts, and 12 of these were diagnosed with idiopathic RV outflow tract tachycardia.

Delayed-enhancement MRI. Figure 1A shows an example of delayed enhancement of the RV anterior wall on an axial MDE-MRI from an ARVD/C patient. Epicardial fat was hyperintense on a non-fat suppressed MDE-MRI, thus making it difficult to distinguish the enhanced RV myocardial signal from that of epicardial fat. Signal in the anterior chest wall close to the cardiac surface coil also contributed to high signal intensity in the anterior mediastinum. Using chemical shift fat-suppression (Fig. 1B) and the body coil instead of the cardiac surface coil (Fig. 1C), the increased signal due to the epicardial fat and cardiac coil were eliminated, and enhancement of the RV anterior wall was confirmed.

Eight of the 12 patients (67%) with a final diagnosis of ARVD/C demonstrated delayed enhancement with MDE-MRI compared with none (0%) of the 18 patients without
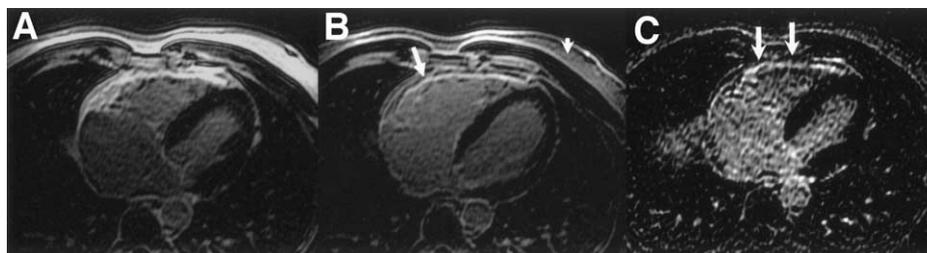

Figure 1. **(A)** This panel shows an axial delayed enhanced image from an arrhythmogenic right ventricular dysplasia patient. The signal intensity of the right ventricular (RV) myocardium is increased, similar to that of epicardial fat. **(B)** This panel shows the same level of the myocardium as **panel A**, using the same pulse sequence with chemical shift fat suppression. The enhanced RV anterior wall is well-appreciated **(arrows)**, and fat in the anterior chest wall has low signal intensity **(arrowhead)**. **(C)** This panel shows the same pulse sequence as **panel B** except that body coil was used for signal transmission and reception. Although the signal-to-noise ratio is decreased compared with surface coil imaging in **panels A and B**, the signal intensity is more uniform across the field of view. This confirms that the RV signal is increased **(arrows)** because of increased myocardial signal rather than proximity to the phased array surface coil.
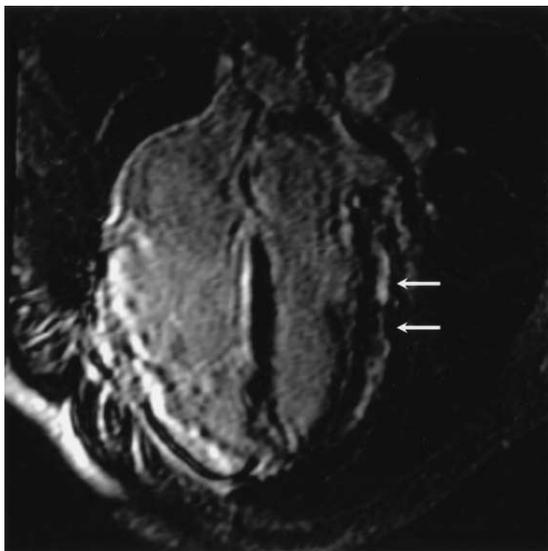
Figure 2. Four-chamber delayed enhanced image from a patient with arrhythmogenic right ventricular dysplasia who had extensive lymphocytic myocarditis on biopsy. The right ventricular (RV) wall and the RV portion of the septum are diffusely enhanced. Further, there is a small area of enhancement in the lateral wall of the left ventricle (LV), possibly indicating LV involvement.

the diagnosis of ARVD/C (p < 0.001). The CNR ratio was significantly higher in the eight patients who had ARVD/C with delayed enhancement compared with the patients who had ARVD/C without enhancement, and the non-ARVD/C patients (10.9 ± 4, −1.5 ± 3.6, and 0.8 ± 2.9, respectively; p < 0.01). The area of delayed enhancement also showed dyskinesis on cine imaging in six of the eight patients (75%).

In six of the eight ARVD/C patients with delayed enhancement, the enhancement was seen in the basal sub-tricuspid region, extending anteriorly into the RV outflow tract. One patient had enhancement of entire anterior wall and the apex; cine images in this patient demonstrated multiple aneurysmal outpouchings of the RV. The same patient also showed diffuse enhancement of the RV portion of the interventricular septum and of the lateral wall of the left ventricle (Fig. 2). A localized area of delayed enhancement that correlated with a small bulging in the outflow tract was observed in one asymptomatic patient with a family history of ARVD/C.

Correlation with endomyocardial biopsy. Endomyocardial biopsy was performed in 9 of the 12 patients who had the final diagnosis of ARVD/C. The remaining three patients refused biopsy. Of these nine patients, four (44%) had fibro-fatty changes consistent with the diagnosis of ARVD/C, one (11%) had extensive myocarditis, and the remainder (44%) had normal biopsies. Each of the four patients with fibro-fatty changes on biopsy had delayed enhancement on MDE-MRI. Of the four ARVD/C patients with normal biopsies, only one had delayed enhancement limited to the antero-basal RV. Endomyocardial biopsy was also performed in 8 (44%) of the 18 patients who did not meet the Task Force criteria for ARVD/C. None of these patients had any abnormalities on histopathology. Also, none of these

patients showed delayed enhancement on MDE-MRI. Presence of delayed enhancement in the RV showed an excellent correlation with fibrosis on biopsy (Fig. 3).

Patients who had delayed enhancement on MRI and who had positive biopsy results (n = 4) had moderate-to-severe RV dysfunction (right ventricular ejection fraction [RVEF] <40%). Three patients with normal RVEF (>55%) who met ARVD/C Task Force criteria had negative biopsies, and one of them had delayed enhancement on MRI. This suggested the possibility of a limited or concealed form of ARVD/C in these patients.

Correlation of delayed enhancement with EP findings. The EP testing was performed in 10 of the 12 ARVD/C patients; 6 had inducible sustained monomorphic VT, and 4 were noninducible (Table 2). The six inducible patients showed delayed enhancement of the RV, compared to only one of the four ARVD/C patients who were noninducible (p = 0.01). Of the 18 non-ARVD/C patients, 12 had EP testing and none of them was inducible for sustained VT. Also, none of these patients had delayed enhancement on MDE-MRI.

Correlation of delayed enhancement on MRI and RV function. The 30 patients were divided into three groups based on number of segments that showed delayed enhancement (<2 segments, 3 to 5 segments, and >5 segments), and the right ventricular end-diastolic volume (RVEDV) and the RVEF were compared between the groups. The mean RVEF decreased (R^2 = 0.82, p < 0.02), while the mean RVEDV showed a significant increase (R^2 = 0.61, p <0.02) with increasing extent of delayed enhancement (Figs. 4A and B).

DISCUSSION

Myocardial delayed enhancement-magnetic resonance imaging is a new but well-validated technique for assessing fibrosis following myocardial infarction (12,13). The identification of fibrosis using this method has not been previously described in ARVD/C. The presence of delayed enhancement showed a high degree of correlation with endomyocardial biopsy and predicted induction of VT during EP testing. Furthermore, there was a strong association between the extent of delayed enhancement and RV dysfunction. These data suggest that MDE-MRI may have an important role in the evaluation and diagnosis of ARVD/C.

Prior studies in ischemic and other nonischemic cardiomyopathies have concluded that the mechanism of delayed enhancement is nonspecific, but may be related to an increase in volume distribution of gadolinium secondary to interstitial space expansion, which occurs in fibrous scarring or inflammation. The histopathologic specimens obtained in our patients with delayed enhancement showed predominantly replacement fibrosis and fat infiltration in the absence of significant inflammation. Most frequently, delayed enhancement was observed in the antero-basal region and in the RV outflow tract, consistent with the previously described anatomic distribution of fibro-fatty infiltration in ARVD/C. In six of the eight ARVD/C patients, regional
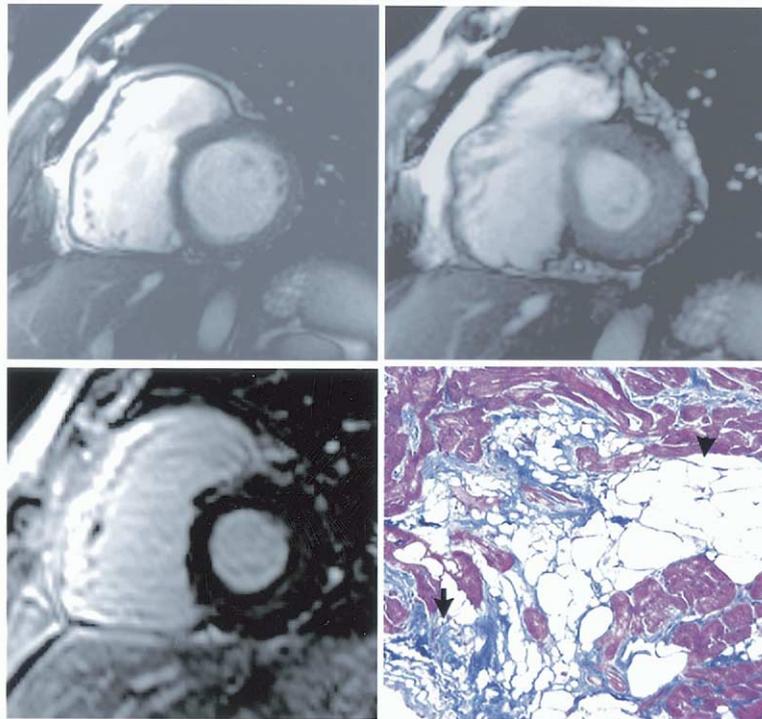
Figure 3. The **top left and right panels** represent the end-diastolic and end-systolic frames of a short-axis cine magnetic resonance image (MRI) showing an area of dyskinesia on right ventricular free wall characterizing a focal ventricular aneurysm **(arrows)**. The **bottom left panel** displays the delayed-enhanced MRI with increased signal intensity within the right ventricular myocardium **(arrows)**, at the location of RV aneurysms. The **bottom right panel** shows the corresponding endomyocardial biopsy. Trichrome stain of the right ventricle at high magnification shows marked replacement of the ventricular muscle by adipose tissue. The adipose tissue cells **(arrowhead)** are irregular in size and infiltrate the ventricular muscle. There is also abundant replacement fibrosis **(arrow)**. There is no evidence of inflammation.

wall-motion abnormalities were observed in the same region, suggesting lack of functioning myocardial cells in the same area. These observations lead us to conclude that the main mechanism of delayed enhancement in ARVD/C may be localization of gadolinium to areas of fibrosis within the RV myocardium. Myocarditis may be yet another mechanism of delayed enhancement in ARVD/C, as in the case of one patient who showed extensive myocarditis with minimal interstitial fibrosis.

Most cases of sustained monomorphic VT are associated with a myocardial scar. Re-entry during EP testing occurs through surviving myocyte bundles in and around the fibrotic areas, which are visualized as contrast-enhanced areas on MDE-MRI. Turrini et al. (15) have previously reported an association between fibrosis on endomyocardial biopsy and the occurrence of sustained ventricular arrhythmias in ARVD/C. Abnormal signal-averaged ECG and reduced RVEF were surrogates for extent of fibrosis in

Table 2. Correlation of MR Myocardial Delayed Enhancement With EP and Histologic Findings in ARVD Patients

| | MR Imaging | | | | EP Testing | | | Histopathology | | |
Case	Fat	Regional Function	MDE	Segments Abnormal	Arrhythmia Morphology	Site	Length (ms)	Fat	Fibrosis	Inflammation
1	ant/RVOT	ant-DK	ant	7	LBBB-SA	apex	260	+	+++	none
2	none	ant-DK	ant	4	RBBB-LA	apex	202	+	+++	none
3	ant/RVOT	ant-DK	diffuse	6	LBBB-IA	RVOT	240	+	+++	+
4	basal	normal	none	0	noninducible	—	—	none	none	none
5	basal	basal DK	basal	3	noninducible	—	—	ND	ND	ND
6	none	RVOT DK	none	0	not done	—	—	ND	ND	ND
7	none	normal	none	0	noninducible	—	—	none	none	none
8	ant/RVOT	basal DK	ant-basal	3	LBBB-IA, LBBB-RA	apex	240,232	none	none	none
9	none	normal	none	0	noninducible	—	—	none	none	+
10	none	ant-DK	ant-basal	1	not done	—	—	ND	ND	ND
11	ant/basal	ant-DK	ant/IVS*	8	LBBB-SA	RVOT	230	none	+	+++
12	ant/RVOT	ant-DK	ant	7	RBBB-LA	RVOT	300	+	+++	+

*Involvement of LV lateral wall.

   ant = RV anterior wall; DK = dyskinesis; EP = electrophysiologic; IA = inferior axis; IVS = interventricular septum; LA = left axis; LBBB = left bundle branch block; LV = Left ventricular; MDE = myocardial delayed enhancement; RA = right axis; RVOT = right ventricular outflow tract.
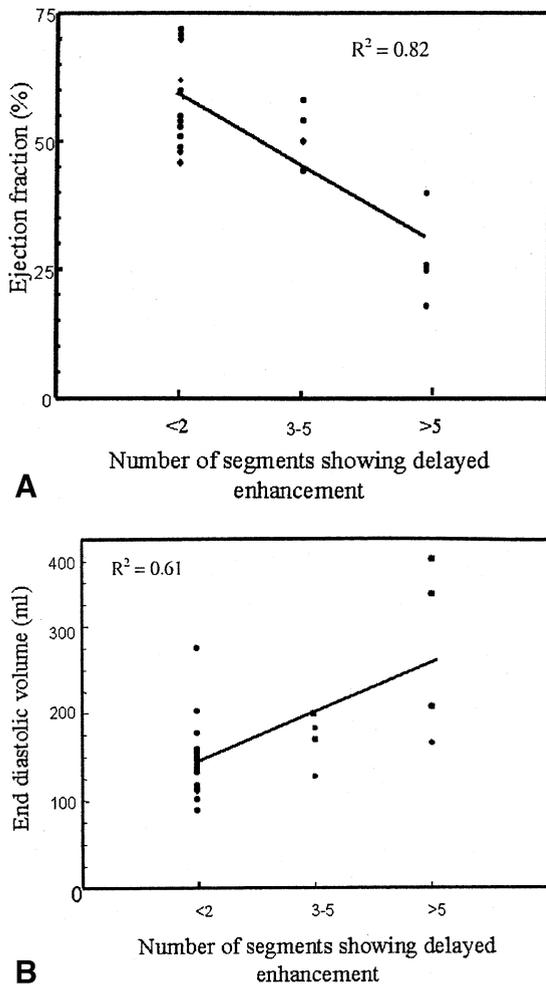
$R^2 = 0.82$

A

$R^2 = 0.61$

B

Figure 4. **(A)** Correlation between the extent of delayed enhancement and right ventricular ejection fraction. **(B)** Correlation between the extent of delayed enhancement and right ventricular end diastolic volume.

to-one basis. The low yield of biopsy (44%) in our study may in fact reflect sampling error or may also be due to the focal nature of the disease process. Another important limitation of our study is the small sample size. Further studies with a large sample size are needed to confirm our results.

Clinical implications. This study suggests for the first time that fibrosis of the RV in ARVD/C can be noninvasively visualized using MRI. The presence of delayed enhancement in ARVD/C was associated with inducibility during EP testing and may also be useful in risk stratification. Abnormal RV enhancement on MRI may help improve the specificity of MRI for ARVD/C diagnosis. The absence of delayed enhancement in each of the patients with idiopathic VT is reassuring, and consistent with the pathophysiology of ventricular arrhythmias in this disease.

Reprint requests and correspondence: Dr. David A. Bluemke, MRI Building, Room 143, Department of Radiology, The Johns Hopkins Hospital, 600 N. Wolfe Street, Baltimore, Maryland 21287. E-mail: dbluemke@jhmi.edu.

REFERENCES

1. Marcus FI, Fontaine G, Guiraudon G, et al. Right ventricular dysplasia: a report of 24 adult cases. Circulation 1982;65:384–98.
2. Fontaine G, Guiraudon G, Frank R, et al. Dysplasie ventriculaire droite arythmogene et maladie de Uhl. Arch Mal Coeur Vaiss 1982;75:361–75.
3. Basso C, Thiene G, Corrado D, et al. Arrhythmogenic right ventricular cardiomyopathy: dysplasia, dystrophy, or myocarditis? Circulation 1996;94:983–91.
4. Corrado D, Basso C, Thiene G, et al. Spectrum of clinicopathologic manifestations of arrhythmogenic right ventricular cardiomyopathy/dysplasia: a multicenter study. J Am Coll Cardiol 1997;30:1512–20.
5. Nava A, Thiene G, Canciani B, et al. Clinical profile of concealed form of arrhythmogenic right ventricular cardiomyopathy presenting with apparently idiopathic ventricular arrhythmias. Int J Cardiol 1992;35:195–206.
6. Angelini A, Basso C, Nava A, et al. Endomyocardial biopsy in arrhythmogenic right ventricular cardiomyopathy. Am Heart J 1996;132:203–6.
7. Ricci C, Longo R, Pagnan L, et al. Magnetic resonance imaging in right ventricular dysplasia. Am J Cardiol 1992;70:1589–95.
8. Tandri H, Calkins H, Nasir K, et al. Magnetic resonance imaging findings in patients meeting task force criteria for arrhythmogenic right ventricular dysplasia. J Cardiovasc Electrophysiol 2003;14:476–82.
9. Fontaliran F, Fontaine G, Fillette F, et al. Nosologic frontiers of arrhythmogenic dysplasia. Quantitative variations of normal adipose tissue of the right heart ventricle. Arch Mal Coeur Vaiss 1991;84:33–8.
10. Globits S, Kreiner G, Frank H, et al. Significance of morphological abnormalities detected by MRI in patients undergoing successful ablation of right ventricular outflow tract tachycardia. Circulation 1997;96:2633–40.
11. Bluemke DA, Krupinski EA, Ovitt T, et al. MR imaging of arrhythmogenic right ventricular cardiomyopathy: morphologic findings and interobserver reliability. Cardiology 2003;99:153–62.
12. Kim RJ, Fieno DS, Parrish TB, et al. Relationship of MRI delayed contrast enhancement to irreversible injury, infarct age, and contractile function. Circulation 1999;100:1992–2002.
13. Kim RJ, Wu E, Rafael A, et al. The use of contrast-enhanced magnetic resonance imaging to identify reversible myocardial dysfunction. N Engl J Med 2000;343:1445–53.
14. Foo TK, Stanley DW, Castillo E, et al. Myocardial viability: breath-hold 3D MR imaging of delayed hyperenhancement with variable sampling in time. Radiology 2004;230:845–51.
15. Turrini P, Angelini A, Thiene G, et al. Late potentials and ventricular arrhythmias in arrhythmogenic right ventricular cardiomyopathy. Am J Cardiol 1999;83:1214–9.

ARVD/C. Consistent with their findings, each of the six ARVD/C patients who had inducible monomorphic VT on EP testing demonstrated myocardial delayed enhancement of the RV. Myocardial delayed enhancement correlated better than abnormal signal-averaged ECG (5 of 6) or RV dysfunction (4 of 6) in predicting VT on EP testing. None of the ARVD/C patients without delayed enhancement was inducible. The above finding highlights the potential of MDE-MRI not only to noninvasively visualize scar tissue, but also to predict the results of EP testing.

In our study, only two-thirds of the ARVD/C patients showed delayed enhancement. The reason for the lack of delayed enhancement in the remainder may be the presence of a pure fatty form of ARVD/C, or may reflect the insensitivity of current MRI techniques to detect a small amount of fibrosis in early disease.

Study limitations. For reasons of safety, biopsy specimens were obtained from an endovascular approach. As such, the biopsy specimens are representative of subendocardial histology only. The location of the biopsies could not be systematically correlated with the MRI findings on a one-